DTU Library

Timoshenko beam element with anisotropic cross-sectional properties

Stäblein, Alexander; Hansen, Morten Hartvig

Link back to DTU Orbit

TIMOSHENKO BEAM ELEMENT WITH ANISOTROPIC CROSS-SECTIONAL PROPERTIES

Alexander R. Stäblein and Morten H. Hansen

[1]Technical University of Denmark, Department of Wind Energy,
Frederiksborgvej 399, DK-4000 Roskilde
e-mail: {alsta,mhha}@dtu.dk

Keywords: Anisotropic Beam Element, Composite Beams

Abstract. *Beam models are used for the aeroelastic time and frequency domain analysis of wind turbines due to their computational efficiency. Many current aeroelastic tools for the analysis of wind turbines rely on Timoshenko beam elements with classical cross-sectional properties (EA, EI, etc.). Those cross-sectional properties do not reflect the various couplings arising from the anisotropic behaviour of the blade material. A two-noded, three-dimensional Timoshenko beam element was therefore extended to allow for anisotropic cross-sectional properties. For an uncoupled beam, the resulting shape functions are identical to the original formulation. The new element was implemented into a co-rotational formulation and validated against natural frequencies and several static load cases of previous works.*

1 INTRODUCTION

Beam models are used for the aeroelastic time and frequency domain analysis of wind turbines due to their computational efficiency. Many current aeroelastic tools for the analysis of wind turbines rely on Timoshenko beam elements with classical cross-sectional properties (EA, EI, etc.). Those beam properties do not reflect the various couplings arising from the anisotropic behaviour of the blade material. The cross-sectional properties of anisotropic beams are commonly expressed in a 6×6 cross-section stiffness matrix. Theories for determining the cross-section stiffness matrix have been presented by e.g. Giavotto et al. [1] and Yu et al. [2]. The method by Giavotto et al. invokes the virtual work per unit beam length to obtain a linear system of second-order differential equations with constant coefficients that have a homogeneous and particular solution. The particular solution is used to determine the 6×6 cross-sectional stiffness matrix. The homogeneous solution is related to warping and is generally ignored. The method by Yu et al. is based on the variational-asymptotic method by Berdichevskii [3].

The anisotropic cross-sectional properties require a suitable beam element for the analysis. Ghiringhelli's [4] element formulation uses the cross-section compliance matrix and beam forces, which vary linearly along length, to obtain the element stiffness by principle of virtual forces. The two-noded element of Kim et al. [5] assumes polynomial shape functions of arbitrary order. The shape function coefficients are determined by minimizing the elastic energy of the beam while satisfying the boundary conditions. Both elements assume small nodal displacements and require a co-rotational or multi-body formulation for geometric nonlinear analysis. A beam element that directly permits large displacement analysis is the mixed variational formulation of Hodges [6].

This paper extends the two-noded, three-dimensional Timoshenko beam element by Bazoune et al. [7]. A cross-section constitutive relationship with a 6×6 stiffness matrix was introduced and the 14 coefficients of the polynomial shape functions were eliminated by two equilibrium equations of the shear force and bending moment relationship and 12 compatibility conditions of the nodal displacements at the element boundaries. With the displacements and rotations known along the beam, the element stiffness matrix was obtained by numerical integration along the element. For an uncoupled beam, where the cross-section stiffness matrix is diagonal, the present formulation is identical to the original formulation. The new element is implemented into a co-rotational formulation by Battini and Pacoste [8] to allow for large displacements and rotations. The anisotropic, co-rotational Timoshenko beam element is validated against natural frequencies and several static cases of previous works. A new test case with a coupled 45-degree bend cantilever is also proposed and compared to results obtained with the beam element by Kim et al. [5].

2 METHODS

In this section a Timoshenko beam formulation for the analysis of anisotropic beams is derived. The present element is an extension of the two-noded, three-dimensional Timoshenko formulation by Bazoune et al. [7] to allow for fully populated 6×6 cross-section stiffness matrices.

2.1 Kinematic Assumptions

The element coordinate system has its origin at the first node of the element. The beam axis x is along the length of the beam, pointing towards the second node. Axes y

and z define the cross-sectional plane of the beam. The lateral displacements u, v and w of the beam axis are expressed as a function of the cross-sectional coordinate x along the element length L. A first order polynomial is assumed for displacement u along the beam axis and third order polynomials are assumed for displacements v and w in the cross-sectional plane.

$$
\begin{align}
u(x) &= c_1 x + c_2 \tag{1}\\
v(x) &= c_3 x^3 + c_4 x^2 + c_5 x + c_6 \tag{2}\\
w(x) &= c_7 x^3 + c_8 x^2 + c_9 x + c_{10} \tag{3}
\end{align}
$$

For torsional displacements along the beam a first order polynomial is assumed

$$
\theta_x(x) = c_{11} x + c_{12} \tag{4}
$$

The rotational displacements θ_y and θ_z around the beam cross section axes follow from Timoshenko's assumption that the curvature of the beam equals the slope plus a contribution from shear deformation

$$
\begin{align}
\theta_y(x) &= -\frac{\partial w}{\partial x} + c_{13} \tag{5}\\
\theta_z(x) &= \frac{\partial v}{\partial x} - c_{14} \tag{6}
\end{align}
$$

To express the displacements and rotations along the beam, the shape function coefficients c_k for $k \in \{1, \ldots, 14\}$ in the equations above have to be determined.

2.2 Constitutive Relations

By introducing the beam strain vector

$$
\varepsilon = \left\{ \frac{\partial u}{\partial x}, \frac{\partial v}{\partial x} - \theta_z, \frac{\partial w}{\partial x} + \theta_y, \frac{\partial \theta_x}{\partial x}, \frac{\partial \theta_y}{\partial x}, \frac{\partial \theta_z}{\partial x} \right\}^T \tag{7}
$$

and the 6×6 cross-section stiffness matrix

$$
\boldsymbol{K}_{cs} = \begin{bmatrix}
K_{11} & K_{12} & K_{13} & K_{14} & K_{15} & K_{16} \\
 & K_{22} & K_{23} & K_{24} & K_{25} & K_{26} \\
 & & K_{33} & K_{34} & K_{35} & K_{36} \\
 & & & K_{44} & K_{45} & K_{46} \\
 & \text{sym.} & & & K_{55} & K_{56} \\
 & & & & & K_{66}
\end{bmatrix} \tag{8}
$$

the cross-section constitutive relation is

$$
\boldsymbol{F} = \boldsymbol{K}_{cs}\, \varepsilon \tag{9}
$$

where $\boldsymbol{F} = \{F_x, F_y, F_z, M_x, M_y, M_z\}^T$ are the beam forces and moments in the cross-section.

3

2.3 Equilibrium and Compatibility

The 14 shape function coefficients c_k are eliminated by introducing two equilibrium equations of the shear force and bending moment relationship

$$\frac{\partial M_y}{\partial x} - F_z = 0, \qquad \frac{\partial M_z}{\partial x} + F_y = 0 \tag{10}$$

and 12 compatibility conditions (6 nodal displacements + 6 nodal rotations) at the element boundaries $x = 0, L$

$$
\begin{aligned}
u(0) &= u_1 & u(L) &= u_2 \\
v(0) &= v_1 & v(L) &= v_2 \\
w(0) &= w_1 & w(L) &= w_2 \\
\theta_x(0) &= \theta_{x1} & \theta_x(L) &= \theta_{x2} \\
\theta_y(0) &= \theta_{y1} & \theta_y(L) &= \theta_{y2} \\
\theta_z(0) &= \theta_{z1} & \theta_z(L) &= \theta_{z2}
\end{aligned}
\tag{11}
$$

where u_n, v_n, w_n and $\theta_{xn}, \theta_{yn}, \theta_{zn}$ for $n = 1, 2$ are the nodal displacements and rotations at the first and second node of the element. With the displacements known along the beam, the elastic energy is

$$V = \frac{1}{2} \int_0^L \boldsymbol{\varepsilon}^T \boldsymbol{K}_{cs} \boldsymbol{\varepsilon} \; dx \tag{12}$$

The element stiffness $\boldsymbol{K}_{el}$ is obtained by creating the Hessian of the elastic energy V with respect to the nodal degrees of freedom.

2.4 Implementation

For implementation in a finite element code the beam element derived above is rewritten in matrix notation. The beam displacements and rotations $\boldsymbol{u}(x) = \{u, v, w, \theta_x, \theta_y, \theta_z\}^T$ of Equations (1) – (6) can be expressed as

$$\boldsymbol{u}(x) = \boldsymbol{A}(x)\boldsymbol{c} \tag{13}$$

where $\boldsymbol{A}(x)$ is the coefficient matrix of the displacements and rotations with respect to the shape function coefficient vector $\boldsymbol{c} = \{c_1, \ldots, c_{14}\}^T$. And similarly for their derivative with respect to the beam axis $\boldsymbol{du}(x) = \{\frac{\partial u}{\partial x}, \frac{\partial v}{\partial x}, \frac{\partial w}{\partial x}, \frac{\partial \theta_x}{\partial x}, \frac{\partial \theta_y}{\partial x}, \frac{\partial \theta_z}{\partial x}\}^T$

$$\boldsymbol{du}(x) = \boldsymbol{dA}(x)\boldsymbol{c} \tag{14}$$

The equilibrium and compatibility Equations (10) and (11) can be written as

$$\boldsymbol{E}(x)\boldsymbol{c} = \boldsymbol{T}\boldsymbol{d} \tag{15}$$

where $\boldsymbol{E}(x)$ is the coefficient matrix of the equilibrium and compatibility equations with respect to the shape function coefficient vector and

$$\boldsymbol{T} = \begin{bmatrix} \underset{2 \times 12}{\boldsymbol{0}} \\ \underset{12 \times 12}{\boldsymbol{I}} \end{bmatrix} \tag{16}$$

is a transformation matrix in which $\underset{2 \times 12}{\mathbf{0}}$ is a 2×12 zero matrix and $\underset{12 \times 12}{\mathbf{I}}$ is a 12×12 identity matrix. The nodal displacements are expressed in the vector

$$\boldsymbol{d} = \{u_1, v_1, w_1, \theta_{x1}, \theta_{y1}, \theta_{z1}, u_2, v_2, w_2, \theta_{x2}, \theta_{y2}, \theta_{z2}\}^T \tag{17}$$

Substituting Equation (15) into (13) and (14), the beam displacements and their derivatives can be expressed as

$$\begin{aligned} \boldsymbol{u}(x) &= \boldsymbol{N}(x)\boldsymbol{d} \tag{18} \\ \boldsymbol{du}(x) &= \boldsymbol{dN}(x)\boldsymbol{d} \tag{19} \end{aligned}$$

where $\boldsymbol{N}(x) = \boldsymbol{A}(x)\boldsymbol{E}(x)^{-1}\boldsymbol{T}$ and $\boldsymbol{dN}(x) = \boldsymbol{dA}(x)\boldsymbol{E}(x)^{-1}\boldsymbol{T}$. Finally, the beam strains $\boldsymbol{\varepsilon}$ are expressed in terms of nodal displacements and rotations

$$\boldsymbol{\varepsilon} = \boldsymbol{B}(x)\boldsymbol{d} = \left[\boldsymbol{dN}(x) + \boldsymbol{T}_N \boldsymbol{N}(x)\right]\boldsymbol{d} \tag{20}$$

where $\boldsymbol{B}(x) = \boldsymbol{dN}(x) + \boldsymbol{T}_N \boldsymbol{N}(x)$ is the strain displacement matrix and

$$\boldsymbol{T}_N = \begin{bmatrix} 0 & 0 & 0 & 0 & 0 & 0 \\ 0 & 0 & 0 & 0 & 0 & -1 \\ 0 & 0 & 0 & 0 & 1 & 0 \\ 0 & 0 & 0 & 0 & 0 & 0 \\ 0 & 0 & 0 & 0 & 0 & 0 \\ 0 & 0 & 0 & 0 & 0 & 0 \end{bmatrix} \tag{21}$$

a transformation matrix. The element stiffness matrix $\boldsymbol{K}_{el}$ of the anisotropic Timoshenko beam element is obtained by numerical integration over the beam length L

$$\boldsymbol{K}_{el} = \int_0^L \boldsymbol{B}(x)^T \boldsymbol{K}_{cs} \boldsymbol{B}(x) \, dx \tag{22}$$

A consistent mass matrix for the above element is obtained from

$$\boldsymbol{M}_{el} = \int_0^L \boldsymbol{N}(x)^T \boldsymbol{M}_{cs} \boldsymbol{N}(x) \, dx \tag{23}$$

where $\boldsymbol{M}_{cs}$ is the cross-section mass matrix containing mass and inertia of the cross-section with respect to the beam displacements and rotations.

3 RESULTS

The proposed element is validated by comparing the results of different test cases with those of previous publications. To allow for large displacements and rotations, the beam element above was combined with an implementation of the co-rotational formulation proposed by Battini and Pacoste [8]. The system was solved using a Newton-Raphson procedure.

3.1 Eigenfrequencies of a coupled cantilever

In the first example, the natural frequencies of a coupled cantilever box beam proposed by Hodges et al. [9] were investigated. The beam is 2.54 m long, has a height of 16.76 mm (0.66 in) and a width of 33.53 mm (1.32 in). The wall thickness is 0.84 mm (0.033 in) with six layers of unidirectional lamina stacked $(20/-70/20/-70/-70/20)$ from outside

to inside. The material is T 300 / 5208 Graphite / Epoxy with properties provided by Stemple and Lee [10]. The material density is given by Hodges et al. as 1604 kg/m^3 ($1.501 \cdot 10^{-4}$ lbsec^2/in^4). The cross-section stiffness matrix was taken from Hodges et al. and converted to SI units

$$\boldsymbol{K}_{cs} = \begin{bmatrix} 5.0576 \cdot 10^6 & 0 & 0 & -1.7196 \cdot 10^4 & 0 & 0 \\ & 7.7444 \cdot 10^5 & 0 & 0 & 8.3270 \cdot 10^3 & 0 \\ & & 2.9558 \cdot 10^5 & 0 & 0 & 9.0670 \cdot 10^3 \\ & & & 1.5041 \cdot 10^2 & 0 & 0 \\ & \text{sym.} & & & 2.4577 \cdot 10^2 & 0 \\ & & & & & 7.4529 \cdot 10^2 \end{bmatrix} \tag{24}$$

The cantilever was discretised with 16 elements. In Table 1 the results of the present model are compared with beam models by Hodges et al. [9] and Armanios and Badir [11] as well as a finite element shell model by Kim et al. [5].

3.2 Tip displacements and rotations of a coupled cantilever

A test case for the static analysis of a coupled cantilever was taken from Wang et al. [12]. The stiffness matrix is provided in the original study as

$$\boldsymbol{K}_{cs} = \begin{bmatrix} 1368.17 & 0 & 0 & 0 & 0 & 0 \\ & 88.56 & 0 & 0 & 0 & 0 \\ & & 38.78 & 0 & 0 & 0 \\ & & & 16.96 & 17.61 & -0.351 \\ & \text{sym.} & & & 59.12 & -0.370 \\ & & & & & 141.47 \end{bmatrix} \cdot 10^3 \tag{25}$$

The beam has a length of 10 m and was discretised by 10 elements. A tip load of 150 N was applied to the cantilever. The tip displacements and rotations (in Wiener-Milenkovic Parameter) are shown in Table 2.

3.3 Curvature and twist of a coupled cantilever

Chandra et al. [13] conduct experiments on box beams with different layups. The cross-section has a dimension of 13.6×24.2 mm (0.537×0.953 inch) with a wall thickness of (6 plies) 7.6 mm (0.03 inch). The length of the cantilever is 76.2 cm (30 inch). The symmetric layup with $(45)^6$ in the flanges and $(45/-45)^3$ in the webs under a tip load of 4.448 N (1 lb.) was chosen for comparison. As the material properties of the AS4/3501-6 Unidirectional Graphite/Epoxy are incomplete in the original publication, the following

Mode	Freq. [Hz]				Rel. Diff. [%]		
	Present	Hodges	Armanios	Kim	Hodges	Armanios	Kim
1 vert.	2.94	3.00	2.96	2.98	2.0	0.7	1.4
1 horiz.	5.07	5.19	5.10	5.12	2.4	0.6	1.0
2 vert.	18.38	19.04	18.54	18.65	3.6	0.9	1.5
2 horiz.	31.72	32.88	31.98	32.02	3.7	0.8	0.9
3 vert.	51.37	54.65	51.92	52.17	6.4	1.1	1.6
3 horiz.	88.43	93.39	89.55	93.39	5.6	1.3	5.6
1 tors.	180.10	180.32	177.05	-	0.1	-1.7	-
2 tors.	542.04	544.47	531.15	-	0.4	-2.0	-

Table 1: Eigenfrequencies of a coupled cantilever obtained with the present model compared to results by Hodges et al. [9], Armanios and Badir [11] (both beam models) and Kim et al. [5] (FEM model).

	u_1	u_2	u_3	θ_1	θ_2	θ_3
Present	-0.09013	-0.06320	1.22950	0.18447	-0.17987	0.00523
Wang	-0.09064	-0.06484	1.22998	0.18445	-0.17985	0.00488
Rel. Diff. [%]	0.57	2.59	0.04	-0.01	-0.01	-6.77

Table 2: Tip displacements and rotations (in Wiener-Milenkovic Parameter) of a coupled cantilever obtained with the present model compared to results by Wang et al. [12].

properties were assumed for this study

$$
\begin{aligned}
E_{11} &= 142 \text{ GPa} & E_{22} &= 9.81 \text{ GPa} \\
G_{12} &= 6.00 \text{ GPa} & G_{23} &= 3.77 \text{ GPa} \\
\nu_{12} &= 0.30 & \nu_{23} &= 0.42
\end{aligned}
\tag{26}
$$

The cross-sectional properties were determined using BECAS, an implementation of the theory by Giavotto et al. [1], as

$$
\boldsymbol{K}_{cs} = \begin{bmatrix}
11.387 \cdot 10^5 & 2.909 \cdot 10^5 & 0 & -30.458 & 12.674 & 0 \\
 & 4.189 \cdot 10^5 & 0 & -11.932 & 8.689 & 0 \\
 & & 3.122 \cdot 10^5 & 0 & 0 & 12.302 \\
 & & & 62.692 & -21.741 & 0 \\
 & \text{sym.} & & & 35.146 & 0 \\
 & & & & & 80.594
\end{bmatrix}
\tag{27}
$$

Smith and Chopra [14] compare the experimental results by Chandra et al. to an analytical formulation and a finite element beam model. Figures 1 and 2 show the slope and twist along the beam obtained with the present model, the experimental results by Chandra et al., and the beam model used by Smith and Chopra. The experimental and beam model data was obtained by digitizing the plots of Smith and Chopra.

3.4 Pre-bend cantilever

This example illustrates a truly three-dimensional response and was initially presented by Bathe and Bolourchi [15]. It comprises a 45° bend cantilever with a radius of 100 m as shown in Figure 3. A square unit cross section with a modulus of elasticity of 10^7 N/m^2 was used. Bend-twist coupling was introduced by setting $K_{45} = -0.3\sqrt{K_{44}K_{55}}$ of the cross-section stiffness matrix. With a tip load of 300 N, the solution converges with 5 iterations on average. Table 3 shows the tip displacement of the uncoupled beam compared to results by Simo & Vu-Quoc [16]. And the coupled beam compared to results obtained with the element proposed by Kim et al. which was implemented in the co-rotational formulation used in the present study.

4 DISCUSSION

A linear Timoshenko beam element with anisotropic cross-sectional properties was derived by extending an existing formulation. The beam model was implemented into a co-rotational formulation to allow for geometric nonlinear analysis and several test cases were analysed. A Python implementation of the proposed beam element, together with the element by Kim et al. and the co-rotational formulation by Battini and Pacoste is available on GitHub [1].

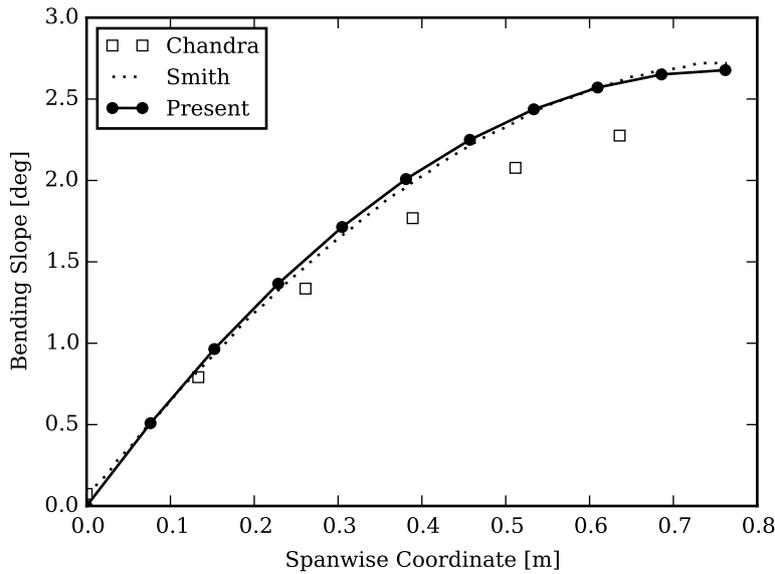[1]https://github.com/alxrs/eccomas_2016.git

Figure 1: Comparison of slope along the beam obtained from experiments by Chandra et al. [13], beam model by Smith and Chopra [14], and present formulation.
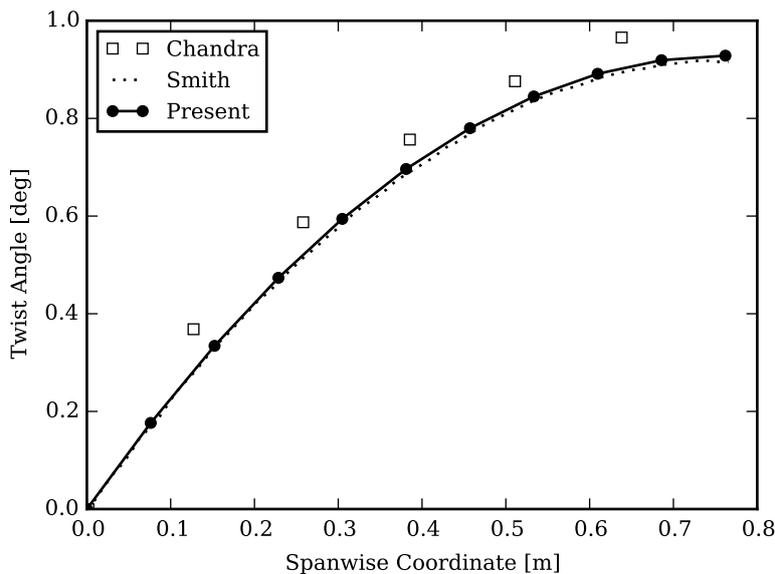

Figure 2: Comparison of twist along the beam obtained from experiments by Chandra et al. [13], beam model by Smith and Chopra [14], and present formulation.

	Displacement [m]			Rel. Diff. [%]		
	x	y	z	x	y	z
Simo & Vu-Quoc	-11.87	-6.96	40.08	-	-	-
Present uncpl.	-12.15	-7.15	40.49	2.3	2.7	1.0
Present cpl.	-10.66	-6.53	38.68	-	-	-
Kim et al. cpl.	-10.66	-6.53	38.70	0.1	0.0	0.0

Table 3: Comparison of pre-bend cantilever tip displacements original and bend-twist coupled beam.
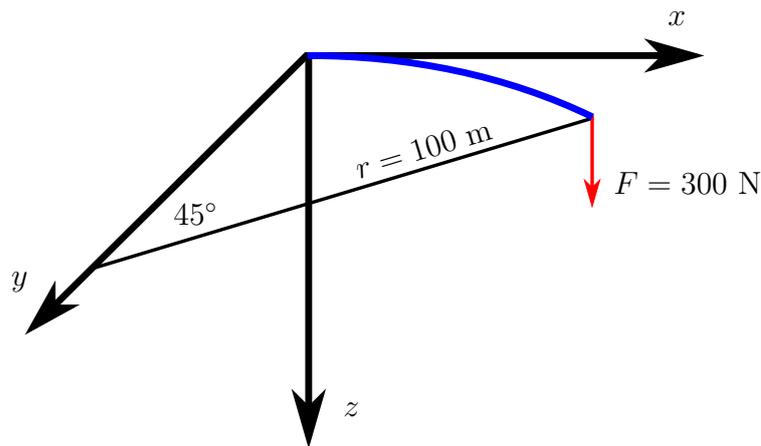
Figure 3: Prebend cantilever.

The present beam element is in good agreement with other formulations. The eigenvalues of a coupled cantilever beam of the first three vertical and horizontal modes and the first two torsional modes are within 2% of another beam formulation and within 6% of a finite element shell model. The tip displacements and rotations of a different coupled cantilever with a tip load are within 3% and 7% of the original study. The curvature and twist along a third cantilever is in good agreement with previous beam model results but deviates somewhat from experiments. The tip displacements of an uncoupled prebend cantilever are within 3% of previous studies. The tip displacements of a coupled prebend cantilever a nearly identical with the results obtained from a different beam element that has been implemented.

ACKNOWLEDGEMENT

REFERENCES

[1] V. Giavotto, M. Borri, P. Mantegazza, G. L. Ghiringhelli, V. Carmaschi, G. C. Maffioli, and F. Mussi. Anisotropic beam theory and applications. *Computers & Structures*, 16(1):403–413, 1983, DOI: 10.1016/0045-7949(83)90179-7.

[2] W. Yu, D. H. Hodges, V. Volovoi, and C. E. Cesnik. On timoshenko-like modeling of initially curved and twisted composite beams. *International Journal of Solids and Structures*, 39(19):5101–5121, 2002, DOI: 10.1016/S0020-7683(02)00399-2.

[3] V. L. Berdichevskii. Variational-asymptotic method of constructing a theory of shells. *Journal of Applied Mathematics and Mechanics*, 43(4):711–736, 1979, DOI: 10.1016/0021-8928(79)90157-6.

[4] G. L. Ghiringhelli. On the linear three-dimensional behaviour of composite beams. *Composites Part B: Engineering*, 28(5):613–626, 1997, DOI: 10.1016/S1359-8368(96)00075-3.

[5] T. Kim, A. M. Hansen, and K. Branner. Development of an anisotropic beam finite element for composite wind turbine blades in multibody system. *Renewable Energy*, 59:172–183, Nov. 2013, DOI: 10.1016/j.renene.2013.03.033.

[6] D. H. Hodges. A mixed variational formulation based on exact intrinsic equations for dynamics of moving beams. *International journal of solids and structures*, 26(11):1253–1273, 1990, DOI: 10.1016/0020-7683(90)90060-9.

[7] A. Bazoune, Y. A. Khulief, and N. G. Stephen. Shape functions of three-dimensional Timoshenko beam element. *Journal of Sound and Vibration*, 259(2):473–480, 2003, DOI: 10.1006/jsvi.2002.5122.

[8] J.-M. Battini and C. Pacoste. Co-rotational beam elements with warping effects in instability problems. *Computer Methods in Applied Mechanics and Engineering*, 191(17):1755–1789, 2002, DOI: 10.1016/S0045-7825(01)00352-8.

[9] D. H. Hodges, A. R. Atilgan, M. V. Fulton, and L. W. Rehfield. Free-vibration analysis of composite beams. *Journal of the American Helicopter Society*, 36(3):36–47, 1991, DOI: 10.4050/jahs.36.36.

[10] A. D. Stemple and S. W. Lee. Finite-element model for composite beams with arbitrary cross-sectional warping. *AIAA journal*, 26(12):1512–1520, 1988, DOI: 10.2514/3.48797.

[11] E. A. Armanios and A. M. Badir. Free vibration analysis of anisotropic thin-walled closed-section beams. *AIAA journal*, 33(10):1905–1910, 1995, DOI: 10.2514/3.12744.

[12] Q. Wang, M. Sprague, J. Jonkman, and N. Johnson. Nonlinear legendre spectral finite elements for wind turbine blade dynamics. In *Proceedings of the 32nd ASME Wind Energy Symposium, National Harbor, Maryland*, 2014, DOI: 10.2514/6.2014-1224.

[13] R. Chandra, A. Stemple, and I. Chopra. Thin-walled composite beams under bending, torsional, and extensional loads. *Journal of Aircraft*, 27(7):619–626, July 1990. WOS:A1990DU94000007, DOI: 10.2514/3.25331.

[14] E. C. Smith and I. Chopra. Formulation and evaluation of an analytical model for composite box-beams. *J. Am. Helicopter Soc.*, 36(3):23–35, 1991, DOI: 10.2514/6.1990-962.

[15] K.-J. Bathe and S. Bolourchi. Large displacement analysis of three-dimensional beam structures. *International Journal for Numerical Methods in Engineering*, 14(7):961–986, 1979, DOI: 10.1002/nme.1620140703.

[16] J.C. Simo and L. Vu‿Quoc. A three-dimensional finite-strain rod model. Part II: Computational aspects. *Computer Methods in Applied Mechanics and Engineering*, 58:79–116, 1986, DOI: 10.1016/0045-7825(86)90079-4.